The Journal of Chemical Physics

Aggregation rate of amyloid beta peptide is controlled by beta-content in monomeric state

Cite as: J. Chem. Phys. **150**, 225101 (2019); https://doi.org/10.1063/1.5096379
Submitted: 17 March 2019 . Accepted: 20 May 2019 . Published Online: 10 June 2019

Tran Thi Minh Thu, Nguyen Truong Co, Ly Anh Tu, and Mai Suan Li

The Journal of Chemical Physics ARTICLE scitation.org/journal/jcp

Aggregation rate of amyloid beta peptide is controlled by beta-content in monomeric state

Cite as: J. Chem. Phys. 150, 225101 (2019); doi: 10.1063/1.5096379
Submitted: 17 March 2019 • Accepted: 20 May 2019 •
Published Online: 10 June 2019

Tran Thi Minh Thu,[1,2,3] Nguyen Truong Co,[4] Ly Anh Tu,[3] and Mai Suan Li[4,a)]

AFFILIATIONS

[1]Institute for Computational Science and Technology, SBI Building, Quang Trung Software City, Tan Chanh Hiep Ward, District 12, Ho Chi Minh City, Vietnam
[2]Department of Metarials Science and Technology, University of Science-VNUHCM, 227 Nguyen Van Cu, District 5, Ho Chi Minh City, Vietnam
[3]Department of Applied Physics, Faculty of Applied Science, Ho Chi Minh City University of Technology-VNU HCM, 268 Ly Thuong Kiet Street, District 10, Ho Chi Minh City, Vietnam
[4]Institute of Physics, Polish Academy of Sciences, Al. Lotnikow 32/46, 02-668 Warsaw, Poland

[a)]**Email:** masli@ifpan.edu.pl

ABSTRACT

Understanding the key factors that govern the rate of protein aggregation is of immense interest since protein aggregation is associated with a number of neurodegenerative diseases. Previous experimental and theoretical studies have revealed that the hydrophobicity, charge, and population of the fibril-prone monomeric state control the fibril formation rate. Because the fibril structures consist of cross beta sheets, it is widely believed that those sequences that have a high beta content (β) in the monomeric state should have high aggregation rates as the monomer can serve as a template for fibril growth. However, this important fact has never been explicitly proven, motivating us to carry out this study. Using replica exchange molecular dynamics simulation with implicit water, we have computed β of 19 mutations of amyloid beta peptide of 42 residues (Aβ42) for which the aggregation rate κ has been measured experimentally. We have found that κ depends on β in such a way that the higher the propensity to aggregation, the higher the beta content in the monomeric state. Thus, we have solved a long-standing problem of the dependence of fibril formation time of the β-structure on a quantitative level.

I. INTRODUCTION

A number of neurodegenerative diseases are believed to be associated with the aggregation of amyloid proteins. For example, according to the amyloid cascade hypothesis, Alzheimer's disease (AD) is caused by the fibrillation of amyloid beta (Aβ) peptides forming amyloid plaques.[1,2] Aβ peptides, which are cleaved from amyloid precursor protein (APP) by β- and γ-secretases, have 36–43 residues, but Aβ40 (40 amino acids) and Aβ42 (42 amino acids) are most abundant. As the main component of amyloid plaques in the human brain, Aβ42 is more neurotoxic than Aβ40 due to faster self-assembly.[3] Because understanding key factors driving protein aggregation is important not only for basic research but also for designing efficient drugs for many diseases, this problem has attracted a lot of attention of researchers in recent decades.

Accumulated experimental and theoretical data indicate that in addition to external factors (pH, T, ionic strength, and protein concentration),[4] there are intrinsic factors such as the hydrophobicity, net charge, secondary structure,[4–7] and chain-length polydispersity[8] and the so-called population of fibril-prone state in monomeric state $\mathbf{N}^*$[7,9] which play a key role in the aggregation propensity. Locking the monomer in a strandlike state by constraining the Asp23-Lys28 salt bridge accelerates the aggregation of amyloid beta peptides considerably.[10,11] As shown by NMR dispersion experiments[12] and simulation,[13] N^* of Fyn SH3 is a nativelike folding intermediate that is prone to aggregation. A high population of fibril-prone state $\mathbf{N}^*$

promotes the formation of template for the protein accumulation leading to an exponential dependence of fibril formation time on the population of this conformation.[7]

The regions enriched by hydrophobic residues promote aggregation[14–17] as evident from the high correlation between the hydration free energy and the aggregation rate of proteins Aβ42, HypF-N, and AcP.[6] Charged residues strongly influence protein aggregation not only because they are involved in specific salt bridges but also because a nonzero net charge prevents self-assembly through repulsion between chains.[18,19]

Chiti and Dobson have demonstrated[5] that the variation in the aggregation rate upon mutation depends on the free energy change in conversion from the α-helix to β-sheet conformation, $\Delta\Delta G = \Delta\Delta G_{\text{coil-}\alpha} + \Delta\Delta G_{\beta\text{-coil}}$. Here, $\Delta\Delta G_{\text{coil-}\alpha}$ and $\Delta\Delta G_{\beta\text{-coil}}$ refer to free energy changes in coil-helix and beta-coil transformations, respectively. However, these quantities were estimated using α-helix and β-sheet propensities of individual wildtype (WT) and mutant residues,[5] leaving the question of the dependence of the fibril formation rate on the monomer β-content open.

In order to clarify the impact of secondary structures on the propensity to aggregation, one has to compute them consistently taking into account the contribution of all residues. To do so, in this paper, we have performed the all-atom replica exchange molecular dynamics (REMD) simulation using the optimized potentials for liquid simulations (OPLS) force field and implicit solvent for the wildtype (WT) and 19 mutants of Aβ42. We showed that the experimentally determined aggregation rate is strongly correlated with the β-content of the monomer, while no correlation with the α-content was observed.

So far, it is believed that the higher the β-content in the monomeric state, the faster the formation of fibrils, but there is no convincing evidence. Here, based on the results obtained for a large dataset, for the first time, we strongly supported this widespread opinion.

II. CHOICE OF SEQUENCES

It is well known that the sequence of a protein controls not only its folding ability but also the propensity to self-assembly.[20,21] Mutation is used to change the sequence resulting in a variation of the aggregation rate.[5] Because the turn region[21–23] of Aβ42, for example, plays a key role in the fibril formation, some mutations, such as Flemish (A21G), Osaka (E22D), Italian (E22K), Arctic (E22G), and Iowa (D23N), have been intensively studied.[18,22,23] Table S1 of the supplementary material lists 19 Aβ42 mutants, for which the aggregation rate has been measured experimentally.[22–24] We will perform a REMD simulation for this set of mutants. Note that by performing 100 ns all-atom conventional MD simulation in explicit water, Chong and Ham showed that the experimentally determined self-assembly rates of these mutants strongly correlate with hydrophobicity in such a way that the higher the hydrophobicity, the faster the aggregation[6] implying the important role of hydration.

III. MOLECULAR DYNAMICS SIMULATION

We have calculated secondary structures of WT and 19 mutants (Table S1 of the supplementary material) in the monomeric state using the OPLS force field[25] and the generalized Born (GB) model for an implicit solvent.[26] The OPLS-AA force field was chosen because for the Aβ monomer it provided conformations consistent with the NMR data.[27] In addition, using this force field in combination with the GB model for water, we previously obtained a reliable estimation of the secondary structures not only of WT but also of mutations of Aβ.[28,29] To improve sampling, REMD was employed with 12 replicas in the temperature range from 290.16 to 490.16 K (see the supplementary material for more details), and for each replica, 500 ns MD simulation was performed. One of the representative structures, obtained in our previous work for the monomer,[28] was chosen as the initial structure for all replicas in WT simulation, while for the mutants we used the same structure but the corresponding mutation was made using the Raptor X web server[30] (Fig. S1 of the supplementary material). Because we used the REMD method, the results should not depend on the starting configuration.

IV. EQUILIBRATION

A. Effectiveness of REMD simulation

To show the effectiveness of REMD simulation, we monitored the evolution of each replica in the replica space. For illustration, we plot the time dependence of exchanges of the second replica with the remaining partners [Fig. S2 (upper panel) of the supplementary material]. Clearly, this replica was exchanged with everyone else, including the farthest 12th, implying that the replica exchange method worked well for our system. This is also confirmed by a strong overlap between adjacent distributions of potential energy of 12 replicas [Fig. S2 (lower panel) of the supplementary material]. For contiguous temperatures, the probability of exchanges is about 20%–30% and this is consistent with the overlap of the potential energy distributions.

B. Time dependence of RMSD, total energy, and beta content

We monitored the time dependence of the root mean square displacement (RMSD), which was calculated using the initial structure as a reference structure and the coordinates of Cα-atoms. We assumed that the system has reached equilibrium when RMSD gets saturation. As evident from Fig. S3 (upper panel) of the supplementary material, the equilibration time is about 210 ns for WT and mutants. This conclusion is further supported by the time dependence of the total energy and beta content of three sequences (Fig. S3 of the supplementary material).

C. Heat capacity in two time windows

To ensure that 210 ns is enough for equilibration, we have computed the specific heat for time windows [210–400] and [210–500] ns using the formula $Cv = (\langle E^2\rangle - \langle E\rangle^2)/(k_B T^2)$, where E is the potential energy and $\langle \ldots \rangle$ denotes the thermodynamics average. The heat capacity, obtained in two time windows at 300 K, for WT, A21G, and E22K, is shown in Fig. S5 of the supplementary material. Since C_V is almost the same for two windows, we conclude that the data were equilibrated. Note that together with WT, we select A21G and E22K as representatives for displaying data because the former is

among the sequences with low β-content, while the latter has the highest β-content (see below). Our result obtained for WT (Fig. S4 of the supplementary material) is consistent with the data reported by Hicks[31] that Cv slightly increases with the temperature in the range of 300–350 K.

D. Secondary structure in two time windows

We have also calculated the secondary structures for the [210–400] and [210–500] ns time windows using the STRIDE algorithm.[32] Since within error the obtained results are identical for these windows (Fig. S5 of the supplementary material), the Aβ42 variants are at equilibrium after 210 ns (see also our previous works for WT[28,29]). The secondary structures obtained in the [210–500] ns window will be used for data analysis. Although the MD simulation has been performed for 12 temperatures, we will consider $T = 300$ K where experimental data were collected. Details of MD simulation are provided in the supplementary material.

V. AGGREGATION RATE DEPENDS ON β-CONTENT

The free energy surface was constructed for Aβ42-WT and two selected mutants A21G and E22K (Fig. S6 of the supplementary material) by using the dihedral angle principle component analysis (dPCA) method in which only the first two important components $V1$ and $V2$ were kept (see the supplementary material for more details). Structures (S) representing major basins clearly show that the mutations alter secondary structures. This is also evident from the per-residue distributions and the most important structures of three sequences shown in Fig. 1. For WT, these distributions were discussed in detail in our previous works.[28,29] For E22K, the β-propensity at the C-terminal levels up compared with WT, while the reduction occurs in this region for A21G. The β-content is compatible in the 18–23 fragment for WT and E22K. Overall, E22K increases the β-content from 21% (WT) to 29%, but A21G reduces it to 13.7% (Table I). This is consistent with the experiments showing that E22K speeds up aggregation, while Flemish A21G slows it down.[6,23]

A. Linear and exponential dependence

Figure 2 shows that the experimentally measured aggregation rate linearly depends on β-content

$$\kappa_{\mathrm{mut}}/\kappa_{\mathrm{wt}} = -0.29 + 0.0635\,\beta, \tag{1}$$

where β is measured in percentage. The correlation level is high as $R = 0.85$. Thus, for the first time, we explicitly showed that the β-content of the monomer controls the aggregation propensity for Aβ peptides and this is expected to be true for other proteins.

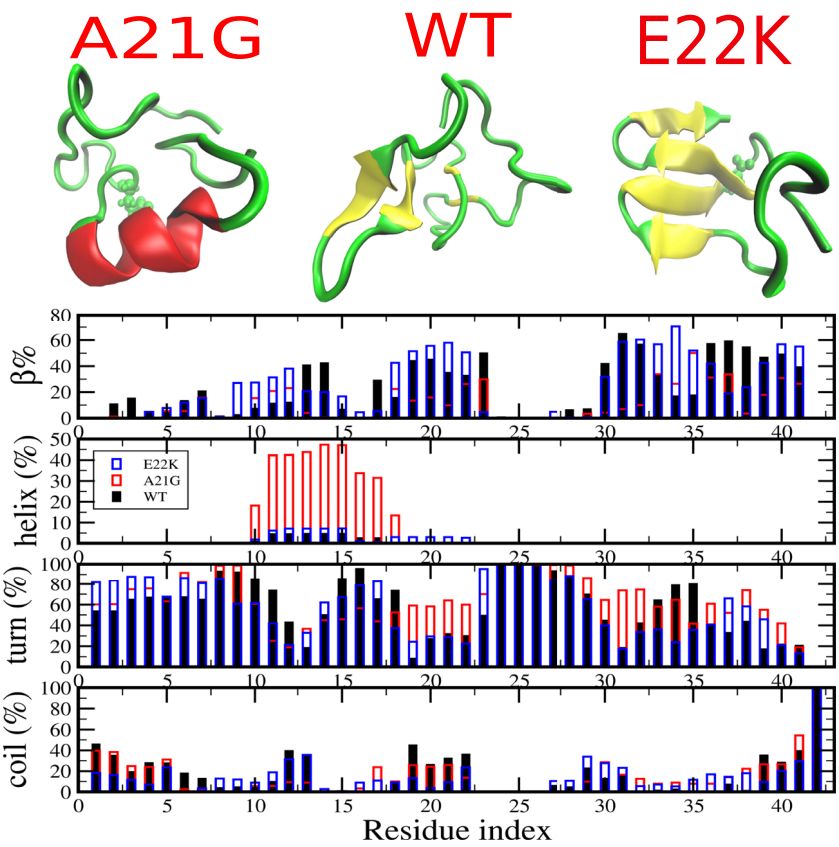

FIG. 1. (Upper) Most representative structures obtained by the clustering method at equilibrium (see structures S1 in Fig. S3 of the supplementary material) for WT, A21G, and E22K. The mutated residue is in the all-atom presentation. (Lower) Per-residue distributions of secondary structures of Aβ42-WT, A21G, and E22K at 300 K. Results were obtained at equilibrium.

TABLE I. The relative computational β-content and observed aggregation propensities of all mutations. The simulation result was obtained at 300 K, the aggregation rate was taken from experiment, and reference is at the last column.

	Simulation		Experiment	
Mutations	β-content (%)	α-content (%)	log (κ_{mut}/κ_{wt})	Reference
Aβ42	20.94 ± 1.91	0.07 ± 1.70	0	
I41D-A42Q	12.92 ± 2.37	1.98 ± 0.47	−0.964	6 and 24
I41D-A42S	12.15 ± 1.93	0.58 ± 0.15	−0.913	
I41H-A42D	11.99 ± 2.38	3.32 ± 0.87	−0.708	
I41E-A42L	13.83 ± 2.32	8.00 ± 2.16	−0.445	
I41H-A42N	15.06 ± 2.85	2.37 ± 0.75	−0.837	
A21G	13.7 ± 2.02	7.63 ± 2.43	−0.671	6 and 23
I41T-A42N	11.82 ± 1.74	0.73 ± 0.21	−0.605	6 and 24
I41T-A42Q	13.31 ± 1.82	0.69 ± 0.30	−0.590	
I41L-A42N	14.61 ± 2.66	0.60 ± 0.14	−0.561	
I41Q- A42L	19.79 ± 3.17	1.35 ± 0.42	−0.295	
I41T-A42M	12.78 ± 1.8	4.72 ± 1.63	−0.292	
I41T- A42I	13.72 ± 1.96	0.26 ± 0.06	−0.075	
I41K	19.00 ± 4.12	0	−0.518	
I41K-A42L	18.56 ± 3.46	3.05 ± 0.72	−0.379	
I41R-A42R	16.54 ± 2.07	3.97 ± 1.39	−0.324	
A42R	15.49 ± 1.9	4.92 ± 1.54	−0.034	
E22G	20.52 ± 2.43	0.67 ± 0.22	0.209	6 and 23
D23N	23.91 ± 2.39	0.80 ± 0.14	0.238	22
E22K	29.06 ± 3.53	1.28 ± 0.36	0.545	6 and 23

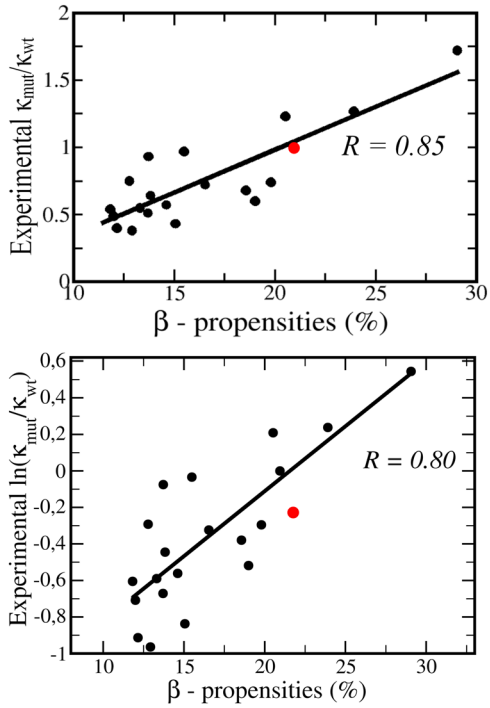

FIG. 2. Dependence of the relative aggregation rate (upper panel) and the logarithm of the relative aggregation rate on the β-content (lower panel). The red circle refers to WT. Linear fits are $y = -0.29 + 0.0635 \times (R = 0.85)$ and $y = -1.534 + 0.071 \times (R = 0.80)$.

Although linear fit [Fig. 2 and Eq. (1)] works well, we can show that the exponential fit is also possible. As evident from Fig. 2, there is also a high correlation ($R = 0.8$) between $\ln(\kappa_{mut}/\kappa_{wt})$ and β-content and their relationship can be described by an exponential function

$$\kappa = \kappa_0 \exp(c\beta), \quad c = 0.071, \tag{2}$$

where κ_0 is a fitting constant and β is measured in percentage. A mutation that levels up self-aggregation enhances the β-propensity in the monomeric state and slows it down otherwise. One can expect that the exponential dependence is valid for other systems as the α-β conversion is a barrier crossing event but constant c may be not universal.

Using lattice models, Li *et al.* have observed the exponential dependence of κ on the population of fibril-prone state $\mathbf{N}^*$.[7] On the other hand, the $\mathbf{N}^*$ conformation is rich in β-sheets implying that the exponential behavior [Eq. (2)] is in the line with this work. From this point of view, exponential fit is more favorable than linear, despite the fact that the correlation of the linear fit is higher. One of the reasons why it is difficult to distinguish two dependences is that the β-content varies in a narrow interval. We have to study a larger dataset to solve this problem.

B. Aggregation rate does not correlate with helix-, turn-, and coil-propensity

At 300 K, the helix-content of Aβ42-WT is practically zero, and the mutations E22K and A21G increase it to 1.28% and 7.63%, respectively (Fig. 1). The enhancement occurs mainly in the 10–18 region. With the exception of I41K, all mutations increase the propensity to helix formation, varying from 0.26 (I41T-A42I) to 8% (I41E-A42L) (Table I). A small change in this quantity as a result of mutations leads to a poor correlation between the self-assembly rate and the α-content (Fig. S7 of the supplementary material, $R = 0.16$). This is also consistent with the experiment showing that Aβ42-WT is much more aggregation prone than Aβ40-WT[33] although they have almost the same helix content.[28]

The turn is highly populated at the C-terminal and in the 22–29 region (Fig. 1). In A21G, it increases mainly at residues 9, 19–21 and 31–34, while a notable reduction occurs at positions 11, 12, and 15–18, which leads to a slight increase from 61.17% (WT) to 63.47% (A21G). Upon E22K replacement, the turn propensity increases at residues 1–3 and 23, but decreases at positions 11–15 and 29–31, resulting in a decline by about 5%. Compared to the α-content, the turn propensity varies over a wider range from 31.81 (D23N) to 73.54 (I41T-A42N) leading to a higher correlation with experiments ($R = 0.46$, Fig. S8 of the supplementary material). The rationale for this observation is that the formation of fibril contacts, such as the Asp23-Lys28 salt bridge, in the turn segment plays a key role in the fibril growth.[10,11] Nevertheless, it cannot be concluded that the turn-propensity controls the aggregation rate as the correlation coefficient remains below 0.5 (Fig. S8 of the supplementary material).

In WT, the coil structure is about 16% (Table S3 of the supplementary material) and it is predominantly populated at several first and last residues (Fig. 1). After mutation, the per-residue distribution changes (Fig. 1), but the total amount slightly changes remaining in the interval of 13%–21% (Table S3 of the supplementary material). Consequently, as in the case of α-content, the coil propensity poorly correlates with the aggregation rate, having R = 0.15 (Fig. S9 of the supplementary material). One of the possible causes of poor correlation with the α- and coil-content is that these structures are poorly populated in the $\mathbf{N}^*$ state.[34]

VI. EFFECT OF CHARGE, HYDROPHOBICITY, AND PROPENSITY TO CONVERSION FROM AN α-HELICAL TO A β-SHEET CONFORMATION

A. Aggregation rate poorly correlates with the free energy for conversion from an α-helical to a β-sheet conformation $\Delta\Delta G$

The change in free energy from the coil to the β-state, $\Delta\Delta G_{\beta\text{-coil}}$, was calculated using the formula $\Delta\Delta G_{\beta\text{-coil}} = 13.64(P_\beta{}^{wt} - P_\beta{}^{mut})$, where $P_\beta{}^{wt}$ and $P_\beta{}^{mut}$ are the β sheet propensities of the wildtype and mutant residues, respectively, and 13.64 is the conversion constant from the normalized scale to the unit kJ/mol, and $\Delta\Delta G_{\beta\text{-coil}}$ is measured in kJ/mol. Using P_β for the 20 amino acids provided in the supplementary material of Chiti and Dobson[5] and in Table I of Street and Mayo,[35] we obtained $\Delta\Delta G_{\beta\text{-coil}}$ for all sequences studied (Table S4 of the supplementary material).

The change in free energy from α-helix to the coil, $\Delta\Delta G_{coil\text{-}\alpha}$, was estimated using the equation $\Delta\Delta G_{coil\text{-}\alpha} = RT\ \ln(P_\alpha{}^{wt}/P_\alpha{}^{mut})$, where $P_\alpha{}^{wt}$ and $P_\alpha{}^{mut}$ are α-helical propensities of the wildtype and mutated sequences at the mutation site, respectively, and gas constant R = 0.008 314 kJ mol^{-1} K^{-1}. The helix percentage was calculated using the AGADIR algorithm (www.http://agadir.crg.es/), and the results are shown in Table S3 of the supplementary material. The free energy of conversion from an α-helical to a β-sheet conformation, $\Delta\Delta G$, is defined as $\Delta\Delta G = \Delta\Delta G_{\beta\text{-coil}} + \Delta\Delta G_{coil\text{-}\alpha}$ and its values are also given in Table S3 of the supplementary material.

As shown in Fig. 3(a), the correlation between the experimental aggregation rates and $\Delta\Delta G$ is quite low ($R = 0.40$), suggesting that the β-content of the monomeric state is a better indicator for the self-assembly propensity compared to the propensity to conversion from the α-helix to the β-sheet conformation. By confining to mutations that do not change the net charge, Chiti and Dobson showed[5] that for a set of 15 sequences, the correlation level between κ and $\Delta\Delta G$ is noticeably higher ($R = 0.71$) than ours. This result seems to contradict our result, but using the entire set of 27 sequences,[5] we obtained $R = 0.41$ (Fig. S10 of the supplementary material) which is close to our value 0.40. From this prospect, our result is consistent with that of Chiti and Dobson.[5] Nevertheless, further study is needed to clarify the correlation with $\Delta\Delta G$.

B. Aggregation rate correlates with the change in the hydrophobicity (ΔHydr) and overall charge (ΔCharge) due to mutation

Following Dobson *et al.*,[5] we calculated the change in hydrophobicity ΔHydr = $\text{Hydr}_{wt} - \text{Hydr}_{mut}$, where Hydr_{wt} and Hydr_{mut} are the hydrophobicity of the wildtype and mutant sequences, respectively. Similarly, a change in the net charge is

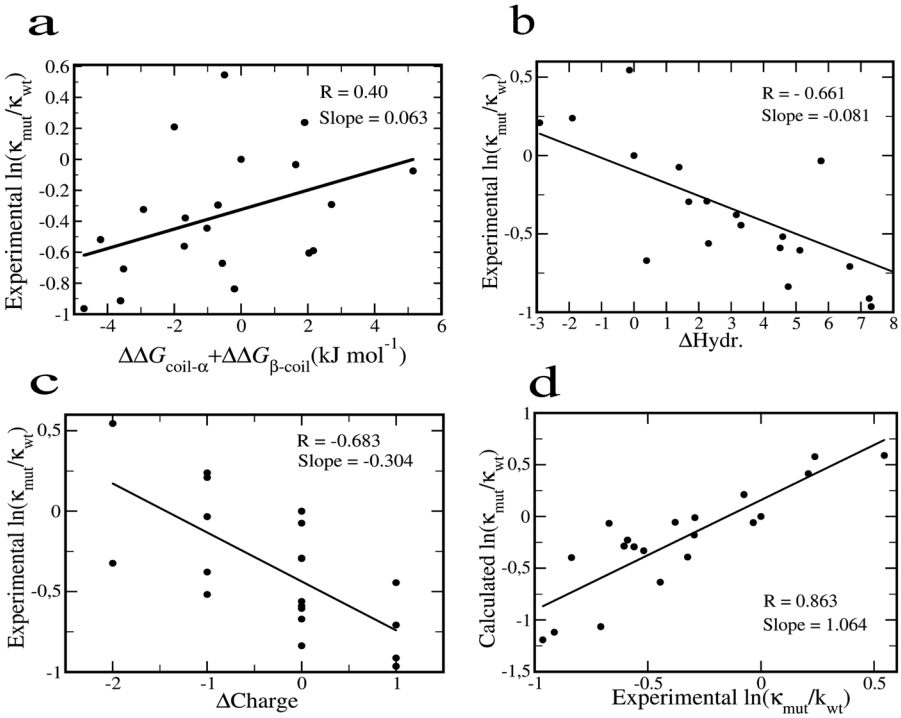

FIG. 3. Dependence of the logarithm of the relative aggregation rate on the predicted change in propensity to convert from an α-helical to a β-sheet conformation (a), hydrophobicity (b), charge (c), and the calculated aggregation rate obtained by Eq. (3) (d). The correlation level and the slope are also shown.

defined as ΔCharge = |Charge$_{mut}$| − |Charge$_{wt}$|, where Charge$_{mut}$ and Charge$_{wt}$ are the charge of the mutation and the wildtype, respectively. We calculated ΔHydr and ΔCharge for all studied sequences (Table S4 of the supplementary material) using the values of hydrophobicity and charge for 20 amino acids provided in the supplementary material of Dobson *et al.*[5]

The level of correlation between the experimental aggregation rate and ΔHydr and ΔCharge is R = 0.661 and 0.683, respectively [Figs. 3(b) and 3(c)]. These values are compatible with 0.545 and 0.721 reported by Dobson *et al.*,[5] but they are noticeably lower than the correlation level between the aggregation rate and the beta content.

We have calculated the change in the aggregation rate due to mutation, using the following equation:[5]

$$\ln(\kappa_{mut}/\kappa_{wt}) = A \cdot \Delta\text{Hydr} + B \cdot \Delta\Delta\text{G} + C \cdot \Delta\text{Charge}. \quad (3)$$

Here, A, B, and C are the slopes obtained from the linear fit between $\ln(\kappa_{mut}/\kappa_{wt})$ and ΔHydr, $\Delta\Delta G$, and ΔCharge, respectively, as follows from Figs. 3(a)–3(c) are −0.081, 0.063 and −0.304, respectively. The predicted aggregation rates, obtained by using Eq. (3), are shown in column 7 of Table S4 of the supplementary material. Despite the poor correlation with $\Delta\Delta G$, its combination with hydrophobicity and charge significantly improves the correlation between the predicted and experimental aggregation rates as we have R = 0.863 [Fig. 3(d)]. This correlation level is as high as that for correlation with the beta content. Interestingly, because the slope in Fig. 3(d) is 1.064 (close to 1), the predicted and experimentally measured rates are almost the same.

VII. CONCLUSION

We have carried out the all-atom REMD simulation in implicit water for various mutations of Aβ42. The correlation between the secondary structures obtained in the monomeric state and the experimentally determined aggregation rates has been thoroughly analyzed. We have found that there is no correspondence between the experimental rate and the helix and coil propensities, while the fit with the turn is relatively poor. Using the data set of 27 sequences from Chiti and Dobson,[5] we demonstrated that if the change in net charge was taken into account, then the experimental κ does not correlate with the propensity to conversion from α-helical to β-sheet conformation free energy $\Delta\Delta G$ as R is below 0.5. One of the possible reasons is that $\Delta\Delta G_{\beta\text{-coil}}$ and $\Delta\Delta G_{\text{coil-}\alpha}$ were determined by the empirical propensities P_β and P_α.[5] A direct estimate of $\Delta\Delta G$ from the all-atom simulation may improve the correlation but this requires for a long simulation that is beyond the scope of this paper. Another possible scenario is that the poor correlation between κ and $\Delta\Delta G$ is due to a small dataset. To clarify this problem, we need more experimental as well as simulation data that are more convincing rather than the existing ones.

We have found a strong correlation between the experimental aggregation rate and β-propensity in the monomer. The dependence of κ on β is expressed by an exponential function in such a way that the higher the β-propensity, the faster the formation of fibril [Eq. (2)]. But linear dependence [Eq. (1)] is not excluded, probably due to the fact that the dataset is not large enough. Nevertheless, our result sheds light on our understanding of major principles that regulate the self-aggregation propensity of proteins, in particular, intrinsically disordered proteins.

Since an estimation of the aggregation rate of long polypeptide chains is beyond existing computational facilities, Eq. (2) [or maybe Eq. (1)] is very useful because it would allow us to predict the aggregation rate based on the β-content, which can be easily obtained by REMD simulation.

SUPPLEMENTARY MATERIAL

See supplementary material for "Material and Method"; initial structure for MD simulation of WT; plots showing the performance of the RE method; time dependence of RMSD, total energy, and beta-content of the three representative sequences; temperature dependence of the heat capacity, per-residue distributions of the beta-content, and free energy surfaces of WT, A21G, and E22K; dependence of the aggregation rate on $\Delta\Delta G$, helix, turn, and coil propensity; tables showing sequences of Aβ42-WT and mutations, characteristics of structures representing major basins on the free energy surface of WT, A21G, and E22K, turn and coil propensities, $\Delta\Delta G_{\beta\text{-coil}}$ and $\Delta\Delta G_{\text{coil-}\alpha}$, estimated for 20 sequences through the β- and α-propensities of amino acids, and ΔHydr and ΔCharge.

ACKNOWLEDGMENTS

This work was supported by Narodowe Centrum Nauki in Poland (Grant No. 2015/19/B/ST4/02721) and Department of Science and Technology at Ho Chi Minh City, Vietnam (Grant No. 19/2017/HĐ-KHCNTT). Allocation of CPU time at the supercomputer center TASK in Gdansk (Poland) is highly appreciated. This research was also supported in part by PLGrid Infrastructure in Poland.

REFERENCES

[1] D. J. Selkoe, Science **275**, 630 (1997).
[2] J. Hardy and G. Higgins, Science **256**, 184 (1992).
[3] D. J. Selkoe, Physiol. Rev. **81**, 741 (2001).
[4] M. Belli, M. Ramazzotti, and F. Chiti, EMBO Rep. **12**, 657 (2011).
[5] F. Chiti, M. Stefani, N. Taddei, G. Ramponi, and C. M. Dobson, Nature **424**, 805 (2003).
[6] S. H. Chong and S. Ham, Angew. Chem. **126**, 4042 (2014).
[7] M. S. Li, N. T. Co, G. Reddy, C. K. Hu, J. E. Straub, and D. Thirumalai, Phys. Rev. Lett. **105**, 218101 (2010).
[8] A. Hernik-Magon, W. Pulawski, B. Fedorczyk, D. Tymecka, A. Misicka, P. Szymczak, and W. Dzwolak, Biomacromolecules **17**, 1376 (2016).
[9] B. Tarus, J. E. Straub, and D. Thirumalai, J. Am. Chem. Soc. **128**, 16159 (2006).
[10] G. Reddy, J. E. Straub, and D. Thirumalai, J. Phys. Chem. B **113**, 1162 (2009).
[11] K. L. Sciarretta, D. J. Gordon, A. T. Petkova, R. Tycko, and S. C. Meredith, Biochemistry **44**, 6003 (2005).
[12] P. Neudecker, P. Robustelli, A. Cavalli, P. Walsh, P. Lundstrom, A. Zarrine-Afsar, S. Sharpe, M. Vendruscolo, and L. E. Kay, Science **336**, 362 (2012).
[13] P. I. Zhuravlev, G. Reddy, J. E. Straub, and D. Thirumalai, J. Mol. Biol. **426**, 2653 (2014).
[14] C. Tanford, Science **200**, 1012 (1978).
[15] K. A. Dill, Biochemistry **29**, 7133 (1990).
[16] A. Ben-Naim, *Hydrophobic Interactions* (Springer Science & Business Media, 2012).
[17] W. Kim and M. H. Hecht, Proc. Natl. Acad. Sci. U. S. A. **103**, 15824 (2006).

[18]F. Chiti, M. Calamai, N. Taddei, M. Stefani, G. Ramponi, and C. M. Dobson, Proc. Natl. Acad. Sci. U. S. A. **99**, 16419 (2002).
[19]A. T. Petkova, Y. Ishii, J. J. Balbach, O. N. Antzutkin, R. D. Leapman, F. Delaglio, and R. Tycko, Proc. Natl. Acad. Sci. U. S. A. **99**, 16742 (2002).
[20]F. Chiti and C. M. Dobson, Annu. Rev. Biochem. **75**, 333 (2006).
[21]J. Nasica-Labouze *et al.*, Chem. Rev. **115**, 3518 (2015).
[22]K. Murakami, K. Irie, A. Morimoto, H. Ohigashi, M. Shindo, M. Nagao, T. Shimizu, and T. Shirasawa, J. Biol. Chem. **278**, 46179 (2003).
[23]C. Nilsberth *et al.*, Nat. Neurosci. **4**, 887 (2001).
[24]W. Kim and M. H. Hecht, J. Biol. Chem. **280**, 35069 (2005).
[25]G. A. Kaminski, R. A. Friesner, J. Tirado-Rives, and W. L. Jorgensen, J. Phys. Chem. B **105**, 6474 (2001).
[26]V. Tsui and D. A. Case, Biopolymers **56**, 275 (2000).
[27]N. G. Sgourakis, Y. Yan, S. A. McCallum, C. Wang, and A. E. Garcia, J. Mol. Biol. **368**, 1448 (2007).
[28]H. L. Nguyen, T. T. M. Thu, P. M. Truong, P. D. Lan, V. H. Man, P. H. Nguyen, L. A. Tu, Y.-C. Chen, and M. S. Li, J. Phys. Chem. B **120**, 7371 (2016).
[29]N. H. Linh, T. T. M. Thu, L. Tu, C.-K. Hu, and M. S. Li, J. Phys. Chem. B **121**, 4341 (2017).
[30]S. Wang, W. Li, S. Liu, and J. Xu, Nucleic Acids Res. **44**, W430 (2016).
[31]D. E. Hicks, "Thermophysical properties of the amyloid beta protein from differential scanning calorimetry," Ph.D. thesis (University of Tennessee, 2005).
[32]M. Heinig and D. Frishman, Nucleic Acids Res. **32**, W500 (2004).
[33]S. W. Snyder, U. S. Ladror, W. S. Wade, G. T. Wang, L. W. Barrett, E. D. Matayoshi, H. J. Huffaker, G. A. Krafft, and T. F. Holzman, Biophys. J. **67**, 1216 (1994).
[34]M. A. Wälti, F. Ravotti, H. Arai, C. G. Glabe, J. S. Wall, A. Böckmann, P. Güntert, B. H. Meier, and R. Riek, Proc. Natl. Acad. Sci. U. S. A. **113**, E4976 (2016).
[35]A. G. Street and S. L. Mayo, Proc. Natl. Acad. Sci. U. S. A. **96**, 9074 (1999).